Ultrastructure of the Intact Skeleton of the Human Erythrocyte Membrane

Betty W. Shen,* Robert Josephs,* and Theodore L. Steck*‡

*Department of Molecular Genetics and Cell Biology, and ‡Department of Biochemistry and Molecular Biology, University of Chicago, Chicago, Illinois 60637

Abstract. Filamentous skeletons were liberated from isolated human erythrocyte membranes in Triton X-100, spread on fenestrated carbon films, negatively stained, and viewed intact and unfixed in the transmission electron microscope. Two forms of the skeleton were examined: (*a*) basic skeletons, stripped of accessory proteins with 1.5 M NaCl so that they contain predominantly polypeptide bands 1, 2, 4.1, and 5; and (*b*) unstripped skeletons, which also bore accessory proteins such as ankyrin and band 3 and small plaques of residual lipid. Freshly prepared skeletons were highly condensed. Incubation at low ionic strength and in the presence of dithiothreitol for an hour or more caused an expansion of the skeletons, which greatly increased the visibility of their elements. The expansion may reflect the opening of spectrin from a compact to an elongated disposition. Expanded skeletons appeared to be organized as networks of short actin filaments joined by multiple (5–8) spectrin tetramers. In unstripped preparations, globular masses were observed near the centers of the spectrin filaments, probably corresponding to complexes of ankyrin with band 3 oligomers. Some of these globules linked pairs of spectrin filaments.

Skeletons prepared with a minimum of perturbation had thickened actin protofilaments, presumably reflecting the presence of accessory proteins. The length of these actin filaments was highly uniform, averaging 33 ± 5 nm. This is the length of nonmuscle tropomyosin. Since there is almost enough tropomyosin present to saturate the F-actin, our data support the hypothesis that tropomyosin may determine the length of actin protofilaments in the red cell membrane.

THE membrane of the human erythrocyte is reinforced at its cytoplasmic surface by a flexible filamentous skeleton composed of spectrin, actin, and band 4.1 (5, 10, 17, 18, 37, 52). This network can be isolated intact and still associated with a set of accessory proteins by dissolving away the overlying lipid bilayer with Triton X-100 (52). The basic skeleton is prepared by stripping away the accessory proteins with molar salt solutions (37). The major accessory proteins are ankyrin, band 3 (and its associated proteins), and band 4.9 (37). Membranes prepared in the presence of Mg^{+2} also contain tropomyosin, presumably bound to the actin (16).

The isolated skeleton contains two major filamentous elements; long, thin, and flexible spectrin molecules and short, thick, and linear protofilaments of actin (5, 10, 17). Spectrin is recovered from ghosts under nondissociating conditions as a mixture of $(\alpha\beta)$ dimers, $(\alpha\beta)_2$ tetramers, and higher oligomers (26). The most prevalent form is the tetramer (26), which measures 194 nm when fully extended (40). Several spectrin filaments are linked to each actin protofilament with junctions stabilized by band 4.1 (12, 30). Band 4.1 also connects the skeleton to the membrane by binding to integral sialoglycoproteins, glycophorins (1, 28). A second set of membrane linkages is provided by ankyrin, which binds both to spectrin and to oligomers of the integral glycoprotein, band 3 (4).

The ultrastructure of the red cell skeleton has been examined by many investigators using a variety of techniques (2, 18, 29, 39, 48, 49). The native structure is so dense, however, that its molecular organization has not been directly visualized. Most of our concepts of the structure of the skeleton derive from the biochemistry and electron microscopy of the isolated proteins (6, 11, 21, 40), recombinants thereof (6, 7, 11), and fragments of the basic network (2, 39). In this work, we have studied the intact skeleton under a variety of conditions selected to reveal features of its native organization.

Materials and Methods

Materials

All chemicals were of reagent grade from Fisher Scientific Co. (Pittsburg, PA), Mallincrodt Inc. (St. Louis, MO), or J. T. Baker Chemical (Allentown, PA). Biochemicals were from Sigma Chemical Co. (St. Louis, MO).

Membranes (ghosts) were prepared as described (15) in 5 mM NaP_i (pH 7.0), sometimes containing 2 mM $MgCl_2$.

Unstripped skeletons were isolated by incubating 1 ml packed ghosts on ice for 1 h in 4 ml of the ghost buffer containing 2.5% Triton X-100 (39, 52).

Stripped skeletons were prepared as described for "skeletons" in reference 39 and in the legend to Fig. 2.

Specimens for electron microscopy were prepared on fenestrated carbon

films atop copper grids according to our previous protocol (39). Two methods of sample application were used; these are described in the legends to Figs. 2 and 4. Electron microscopy was done as before (39). Our criteria for satisfactory preparations included not only the clarity of the image but the uniformity of the field and the reproducibility of the experiment, so that the micrographs presented, while selected, are representative of the experiments described.

Results and Discussion

Skeletons prepared by extracting ghosts with Triton X-100 in 5 mM NaP_i (pH 7.0) contained proteins essential to the integrity of the basic network (bands 1, 2, 4.1, and 5) as well as residual lipid and several accessory proteins (notably, band 2.1, a portion of band 3, band 4.2, and band 4.9; see Fig. 1, gel *B*). Stripping these skeletons at high ionic strength eluted the accessory proteins and the lipid segments linked to them, leaving the basic skeleton with a trace of band 4.9 (see Fig. 1, gel *H* and reference 37).

Ultrastructure of the Basic Skeleton

Fig. 2 shows an image of a portion of a stripped skeleton. It is seen to be a highly expanded, well-spread, single-thickness, irregular network composed of two types of interconnected filaments. One type of filament was shorter (25–75 nm), thicker (~7–8 nm), and more linear than the other; it has been identified as F-actin (39). The other type of filament was long and thin; while it rarely extended to 200 nm, it clearly corresponds to spectrin tetramers (6, 11, 21, 40). A sense of orientation (here, to the horizontal) was often observed in both the spectrin and actin filaments in such preparations. We ascribe this effect to the action of anisotropic surface forces on these highly deformable networks. Multiple spectrins were associated with each protofilament at irregular intervals. Some actin protofilaments showed thickening at the site of association with spectrin filaments. Band 4.1, which stabilizes the spectrin–actin interaction, may be located at these junctions (5, 10, 17). As before (39), globules or discs of ~15-nm diam were also associated with multiple spectrin filaments. There was no apparent regularity to the spacing of either the actin or spectrin filaments. The spectrin filaments tended not to cross one another and frequently ran in parallel between adjacent actin filaments. Neither oligomers of spectrin (26) nor bundles of actin (41) were identified, but they would have been difficult to observe in these preparations.

Exposure of stripped skeletons to glutaraldehyde, isotonic saline, or a combination of the two promoted their condensation. The condensation in glutaraldehyde seemed to reflect extensive lateral aggregation of neighboring spectrin filaments into fibers, while the elevation in ionic strength seemed simply to promote the collapse of the hyper-expanded networks seen in Fig. 2. The combination of glutaraldehyde and isotonic saline led to a honeycomb pattern of thick strands. These images resembled those of earlier studies in which skeletons were exposed to glutaraldehyde and/or acidic pH (18, 29, 48).

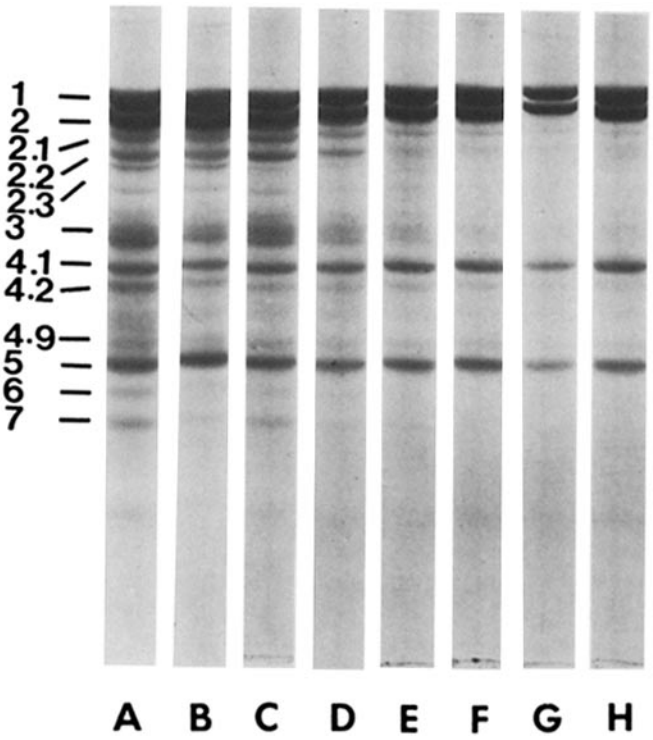

Figure 1. Electrophoretic pattern of the polypeptides of ghosts, unstripped skeletons, and stripped skeletons. Ghosts (*A*) were prepared in 5 mM NaP_i (pH 7.0), extracted with 4 vol of 2.5% Triton X-100 in the same buffer, and the unstripped skeletons pelleted (*B*). The skeletons were then extracted for 5 min on ice with 10 vol of 5 mM NaP_i that contained the following molar concentrations of NaCl: *C*, 0.25; *D*, 0.5; *E*, 0.75; *F*, 1.0; *G*, 1.25, and *H*, 1.5. The residues were pelleted, washed twice in 5 mM NaP_i (pH 7.0), and electrophoresed as described (15). Bands 1 and *2* comprise spectrin; bands *2.1*, *2.2*, and *2.3* are collectively called ankyrin; and band *5* is actin (5, 10, 17).

Ultrastructure of the Unstripped Skeleton

The excessive manipulations required for the preparation of stripped skeletons could have resulted in changes in their molecular organization. We therefore examined skeletons closer to the native state. In early studies, we affixed intact red blood cells to fenestrated carbon films and extracted them in situ with Triton X-100. This procedure yielded skeletons that were too often obscured by the high concentration of hemoglobin. When ghosts were prepared in 5 mM NaP_i (pH 7.0), adsorbed to the carbon film, and then extracted with Triton X-100 in 5 mM NaP_i (pH 7.0), the residual skeletons were quite dense and contained an excessive amount of lipid. Skeletons from ghosts extracted in suspension and applied to the film in 0.15 M NaCl-5 mM NaP_i (pH 7.0) formed circular disks with a diameter of ~6 μm, much smaller than that of the parent membrane (19, 23). (A flattened red cell membrane with an area of 140 μm^2 [9] would form a double-layered disk of diameter 9.4 μm.) These networks were too dense to be interpreted.

We discovered that skeletons incubated in low ionic strength buffer on ice expanded progressively over the course of an hour. Longer incubations did not cause further dilation and risked dissociation of the proteins. (In retrospect, we note that the prolonged dialysis of stripped skeletons against 2 mM NaP_i to remove the concentrated NaCl/sucrose solution had a similar dilating effect [Fig. 2 in reference 39].) We also found that we could apply these specimens directly to the carbon film simply by lowering the detergent concentration by dilution to 200 vol. Since the presence of detergent permitted buffer to flow through the tiny fenestrations in the carbon film, the highly diluted skeletons could be collected and mounted rapidly, thoroughly rinsed, and stained within 3 h of hemolysis.

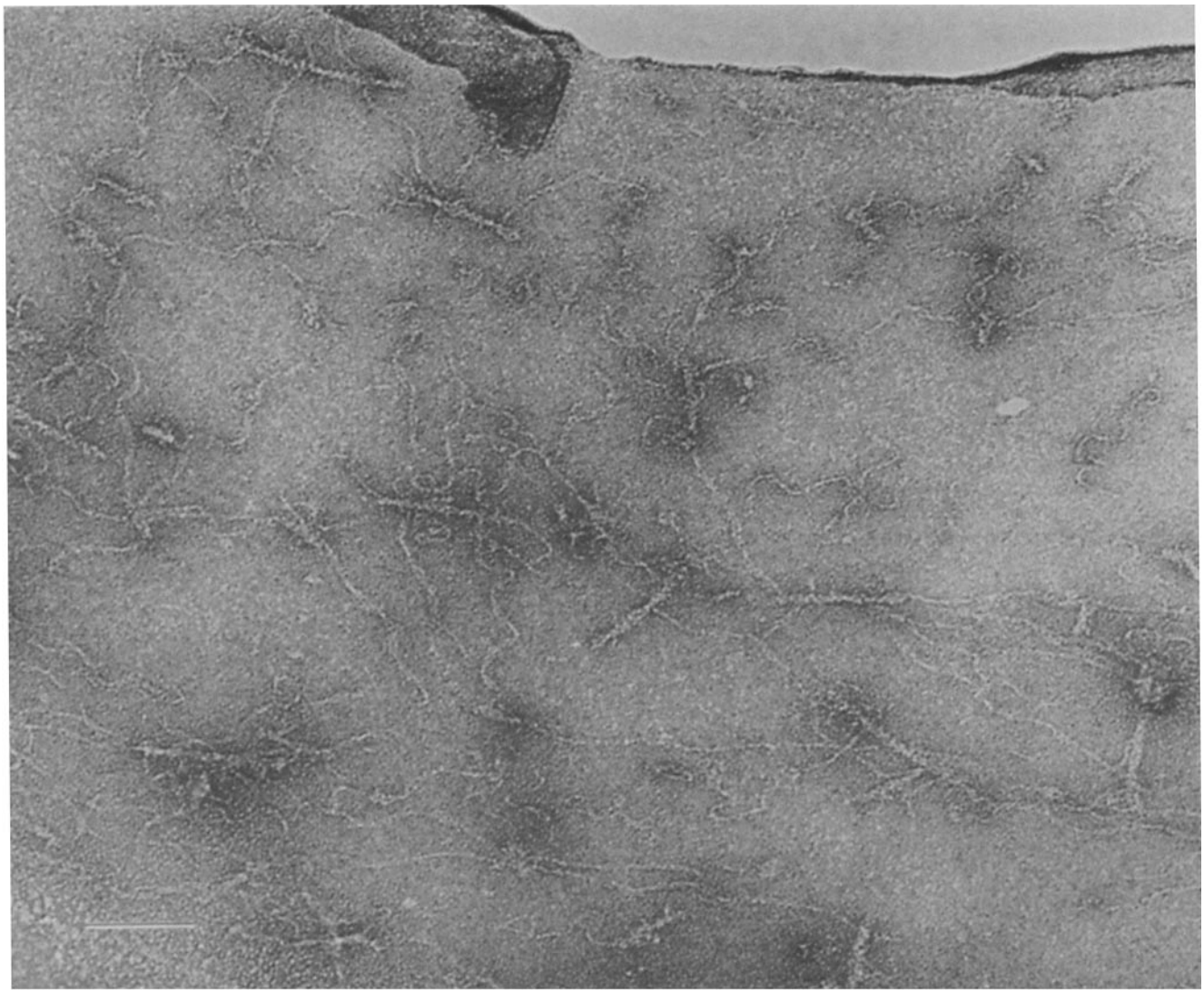

Figure 2. The basic red cell skeleton, stripped and expanded. Ghosts were extracted with 4 vol of 2.5% Triton X-100 in 5 mM NaP_i (pH 7.0) on ice for 1 h. The mixture was layered on a compound density barrier of 10 ml 10%, 10 ml 30%, and 7 ml 60% sucrose (wt/wt) in 1.5 M NaCl-5 mM NaP_i (pH 7.0) and spun at 13,500 rpm for 30 min in an HB-4 rotor (36). The skeletons recovered from the 30%/60% sucrose interface were dialyzed at 5°C overnight against 2 mM NaP_i (pH 7.0) containing 0.5 mM dithiothreitol. One drop of this suspension (~0.3 mg protein/ml) was spread on a fenestrated film on ice for 1 min, the excess drained by capillarity, and the grid quickly rinsed with 2 drops of 1% uranyl acetate and incubated with a final drop for 15 s at room temperature before draining away the excess and drying in air. Bar, 50 nm.

Initially, 2 mM $MgCl_2$ was present in the buffer from the outset to stabilize skeletons and prevent the dissociation of tropomyosin. These skeletons were ~8 μm in diameter, slightly smaller than the native red cell. Their fine structure is illustrated in Fig. 3*a*. The networks were condensed and lacked elongated filaments. The major structural elements were globules and short, thick, linear segments in a coarse irregular reticulum. While these structures cannot be identified unambiguously, they would appear to be a compact version of spectrin, given their abundance and the paucity of spectrin in its familiar filamentous form. While there were a few thin filaments present, they disappeared within 50 nm into the complex conglomerates. Finally, circular plaques of lipid of varied size were attached to the reticulum.

While structures such as that shown in Fig. 3*a* may be the most native we have examined, they did not yield all of the information we desired. We therefore reduced the concentration of $MgCl_2$ in the hour-long incubation to 0.05 mM. As a result, the skeletons expanded to ~11 μm, and their fine structure became clearer (Fig. 3*b*). Globules and short thick filaments were again the most common elements in the reticulum, even on the faces of the associated lipid segments (e.g., lower left portion of *b*). In addition, thin, linear filaments up to 50 nm in length ran between the compact clusters. We infer that the spectrin in these preparations is in two forms: partially elongated or condensed. However, the spectrin is not convoluted as when one or both of its ends are free (2, 6, 11, 26, 39, 40). We imagine that the spreading forces on the carbon film were strong enough to draw the uncondensed segments of spectrin filaments into a linear contour, but were insufficient to expand the condensed regions which must then have a significant strength of self-association.

The addition of 0.5 mM dithiothreitol to the 0.05 mM $MgCl_2$ buffer caused further expansion of the skeleton disks to ~15-μm diam; this corresponds to a surface area more than twice that of the erythrocyte. (The reducing agent may have

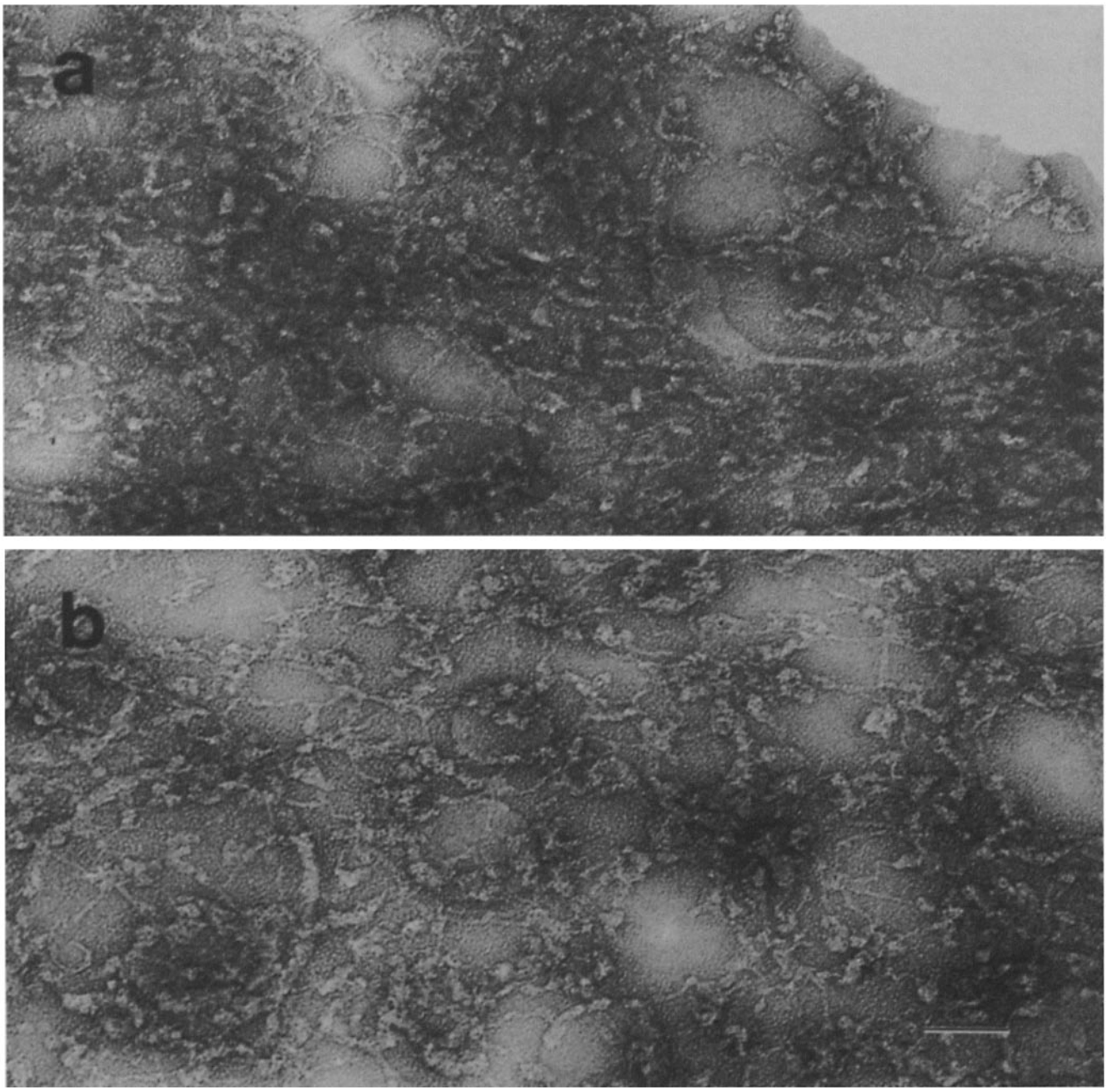

Figure 3. The unstripped skeleton: expansion during preparation. (*a*) Ghosts were prepared from fresh erythrocytes in 5 mM NaP_i (pH 7.0) containing 2 mM $MgCl_2$. 1 vol of ghost was extracted with 4 vol of 5 mM NaP_i (pH 7.0) that contained 2.5% (wt/vol) Triton X-100 and 2 mM $MgCl_2$ for 1 h on ice. The mixture was then diluted to 200 vol in the same buffer that lacked detergent and was incubated for an additional hour on ice. A drop of the suspension was applied slowly to a fenestrated carbon film at room temperature. The skeletons adhered and the fluid flowed through the film to a filter paper wick. The film was then washed with ten drops of water at room temperature over a few seconds and stained as in Fig. 2. (*b*) As in *a*, except that $MgCl_2$ was omitted from the buffer used for the final dilution. (*c–e*) As in *b*, except that the buffer used for the final dilution contained 0.5 mM dithiothreitol. The arrowheads in *c–e* indicate six actin protofilaments; the asterisks indicate two (or possibly three) globular complexes on spectrin filaments. Bar, 50 nm.

acted through its ability to counter the self-association of spectrin [3].) This dilation further clarified the fine structure of the network (Fig. 3, *c–e*). Segments of thin filaments (presumably spectrin) now extended linearly for up to 100 nm between the dense conglomerates, and individual spectrin–actin junctions were visible. We believe that these images are valuable, because they reflect a structure of the skeleton that differs from the native form primarily in being more expanded.

The ultrastructure of the unstripped skeletons represented in Fig. 3, *c–e* differed from that of stripped skeletons (Fig. 2 and reference 39) in several respects: (*a*) Circular plaques of lipid were adherent to the unstripped skeleton (see also references 37 and 52). Presumably, the integral proteins, band 3 and glycophorin, were bound to the unstripped skeletons through ankyrin and band 4.1 and held fast to bits of the bilayer. (*b*) The unstripped skeleton was more densely packed than the stripped skeleton, probably for several reasons. First,

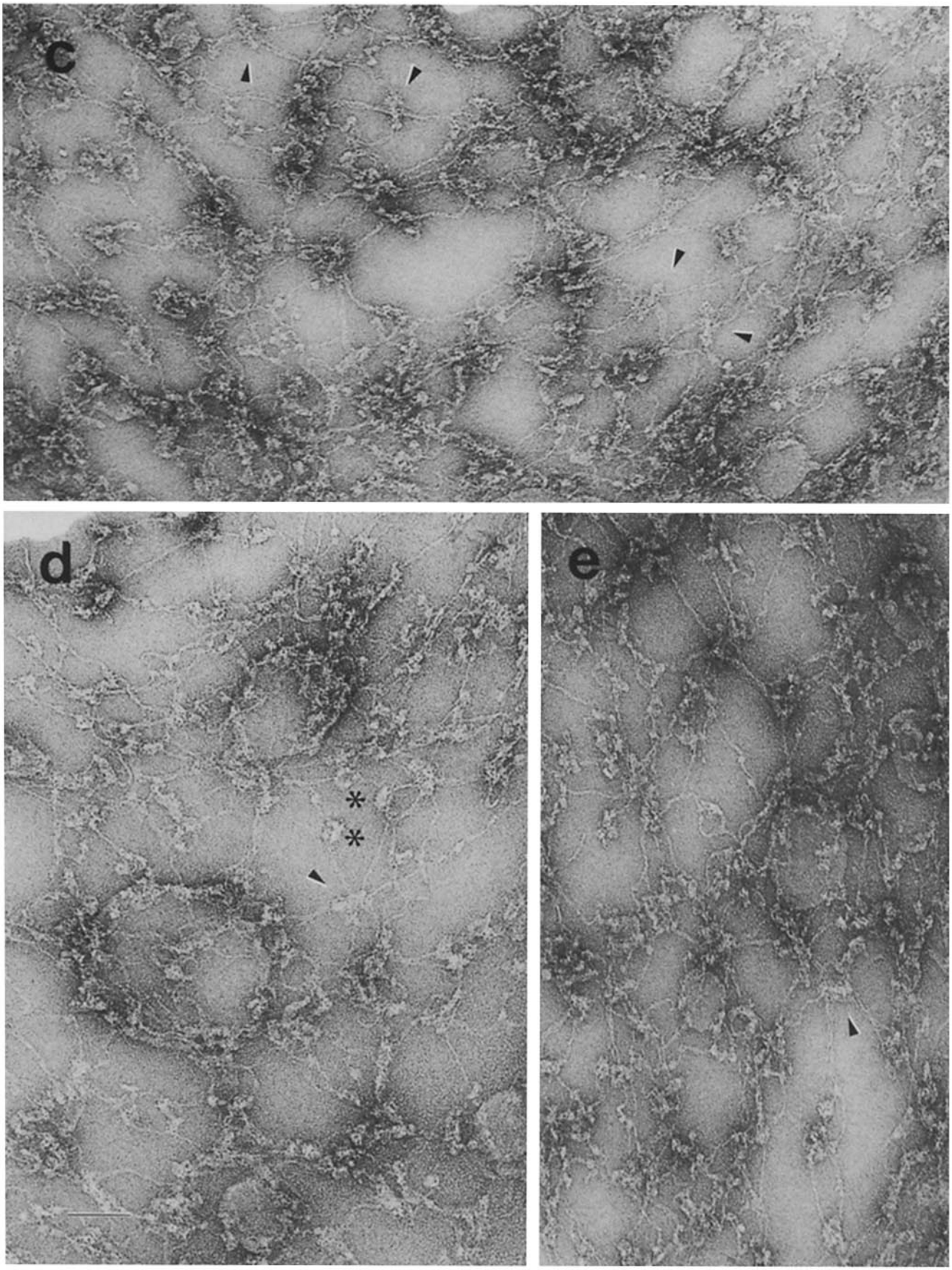

Figure 3.

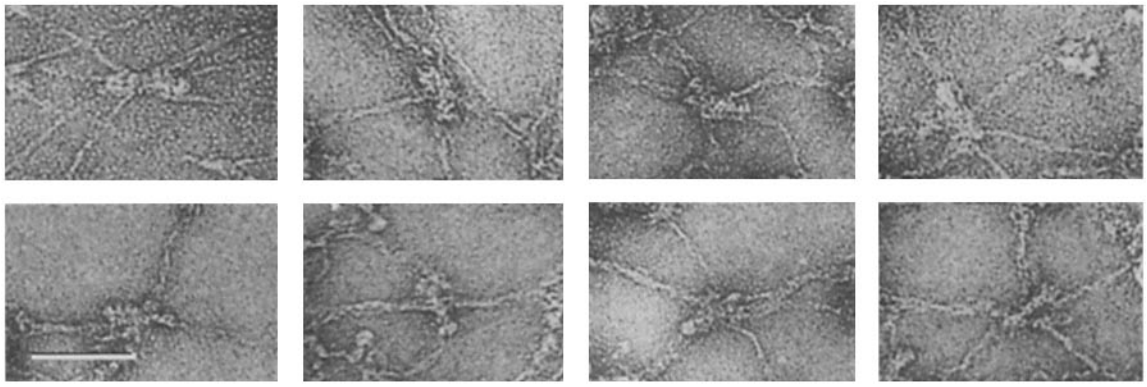

Figure 4. A gallery of actin protofilaments from unstripped skeletons. Skeletons were prepared and photographed as in Fig. 3, *c–e*.

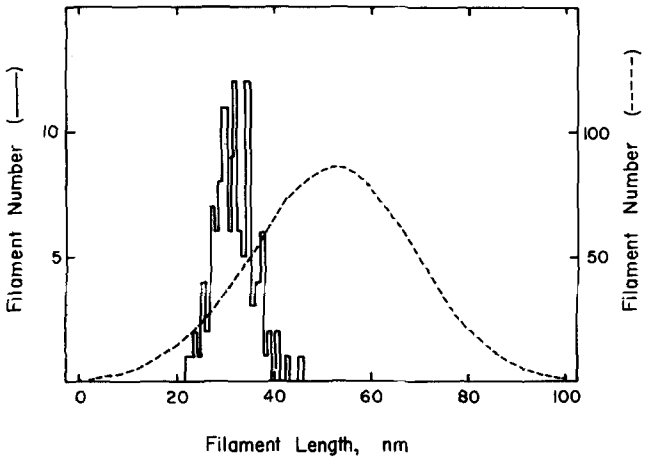

Figure 5. Length of actin protofilaments from unstripped skeletons. Several enlarged prints of micrographs of preparations such as those shown in Fig. 3, *c–e* and Fig. 4 were surveyed, and the length of every filament meeting the four criteria stipulated in the text was measured with a micrometer. A histogram of the length distribution of 138 actin protofilaments was plotted as the solid line. For comparison, the results of a previous analysis of the actin protofilaments in preparations of fragments of the stripped skeleton (38) are shown as the dashed line.

it contained more material (Fig. 1). Second, the unstripped skeletons are probably two-ply (a net collapsed on itself), whereas networks such as that shown in Fig. 2 seem to have been torn open during the washing of the carbon film with water (39). Third, the unstripped networks were less expanded than the stripped networks. We ascribe this to the extra time and extent of processing of the stripped skeletons at low ionic strength. Fourth, the lipid plaques in the unstripped skeleton served as gathering points for the filaments and thereby held them in closer array. (*c*) Extra globular particles, ~15–20 nm in diameter, were observed near the centers of spectrin tetramers (see, for example, the globules marked by asterisks in Fig. 3*d*). These masses are likely to contain complexes of band 2.1, band 3, band 4.2, and band 6, the major proteins present in unstripped but not stripped skeletons (Fig. 1). It has been shown that band 2.1 and hence the band 3, which is associated with it, bind to spectrin in vitro at this position (5, 6, 10, 11, 17), and that bands 4.2 and 6 bind to band 3 (53). (*d*) The actin protofilaments appeared to be thicker and shorter than in the stripped skeletons, with an irregular profile but a rather uniform length (compare segments marked by arrowheads in Fig. 3, *c–e* with Fig. 2 and reference 39). We ascribe the thick and irregular profile of the filaments to the presence of extra material. Specifically, band 4.1 is believed to reside exclusively at spectrin/actin junctions (5, 6, 10, 11, 17) and its total mass is approximately three-fourths that of red cell actin (Fig. 1 and references 31 and 43). In addition, band 4.1 may retain glycophorin with its associated detergent and/or lipid molecules (1, 28). Finally, band 4.9 may add further to the decoration of the protofilaments in the unstripped skeleton (41).

Actin Protofilaments in the Skeleton

The length of actin protofilaments in unstripped skeletons was measured in preparations such as that shown in Fig. 3, *c–e*. To do this, we assessed every structure in several micrographs that fulfilled the following four criteria: (*a*) linearity; (*b*) association with multiple spectrin filaments; (*c*) both ends clearly demonstrable; and (*d*) a thickness of 5–10 nm. A gallery of such structures is shown in Fig. 4. We note in passing that the actin protofilaments are thickened, and the ends of many are bulbous. In addition, each actin protofilament is typically associated with 5–8 spectrin filaments. The junctions with spectrin are found both near the ends and at the center of the actin filaments. The panel in the upper right shows a globular mass on a spectrin filament.

The distribution of the length of such actin protofilaments is shown in Fig. 5 (solid line). The dashed line shows the results of a similar survey of F-actin protofilament lengths in fragments of the stripped skeleton (39). There are two conspicuous differences between these distributions: the actin protofilaments in the unstripped skeletons are shorter than in the stripped skeleton fragments (the mean lengths being 33 and 52 nm) and are less dispersed (the standard deviations being 5 nm and 15 nm, respectively). A 33-nm filament would contain 12 actin subunits (14). This value agrees well with calculations based on estimates of the number of cytochalasin B binding sites ($3–4 \times 10^4$; reference 24) and the number of actin monomers per cell ($2.5–5.0 \times 10^5$; references 31, 38, and 43).

Since the unstripped skeletons have been far less manipulated, we suspect that their F-actin is likely to be closer to the native form than that in the stripped skeletons. In particular, the stripped skeletons (Fig. 2) and their fragments (39) have been exposed to both very high and very low ionic strength solutions as well as sucrose density gradient centrifugation and prolonged dialysis, all in the absence of Mg^{+2}. These

manipulations may have both promoted the dissociation of actin-stabilizing proteins and stimulated the migration of actin monomers from one filament to another (22, 31). Indeed, there is a second population of actin oligomers in the fragments of the stripped skeletons: globules up to 15 nm in diameter that bear multiple spectrins and can nucleate actin polymerization (39). It seems likely that those globules are the remains of longer actin filaments that were eroded to a minimal size by the migration of monomers to longer actin filaments, perhaps in the low ionic strength dialysis step (22). This process would explain the results shown in Fig. 5.

The length of the actin protofilaments in the unstripped skeletons, 33 nm, corresponds precisely to the periodicity or axial repeat along the length of tropomyosin paracrystals from nonmuscle cells (13, 27). Tropomyosin in isolated human red cell membranes has a molecular weight comparable to other nonmuscle species and an abundance of one molecule per 7–8 actin monomers (16). This is enough to provide almost every 33-nm actin filament with a strand of tropomyosin in each of its two helical grooves. Thus, our data support the hypothesis that individual tropomyosin molecules may both stabilize (16) and determine the length of the actin protofilaments.

The ultrastructure of the unstripped skeletons was further clarified by adding one more step to the procedure illustrated in Fig. 3, *c–e*: the skeletons adherent to the fenestrated carbon films were washed vigorously with a continuous stream of distilled water just before staining. As shown in Fig. 6, this treatment expanded the skeletons to a degree comparable to that seen in Fig. 2 for basic skeletons. In addition the nonadherent portion of the networks overlying that affixed to the film was apparently removed (39). As in Fig. 3, *c–e*, the skeletons in Fig. 6 have globular particles in the middle of extended spectrin filaments, circular plaques of adherent lipids (stars), and short, thick actin protofilaments (arrowheads). Spectrin filaments did not intersect one another and seemed to link only adjacent actin filaments. Long, linear, but well-visualized spectrin filaments typically measured between 100 and 150 nm and rarely approached 194 nm, the length ascribed to the fully extended spectrin tetramer (40). Neither higher oligomers of spectrin (26) nor bundles of actin (41) were identified, but neither can be excluded.

A particularly interesting structure is seen in Fig. 6*b*: a pair of spectrin filaments running between common points on adjacent actin protofilaments (arrowheads *1* and *2*) are straddled by two globular masses (asterisks *1* and *2*), each slightly removed from the midpoints of the spectrin tetramers. The globular masses are neither symmetrical nor uniform but contain substructure. Given current concepts of the associations between accessory proteins and the skeleton (5, 10, 17), we suggest that each globule is bivalent, composed of two ankyrin molecules linked to a band 3 oligomer (4, 5). Indeed, starred globule *2* appears to contain a pair of small round bodies, each on a spectrin, joined by a more elongated structure. Similarly, the spectrin tetramer associated with the actin protofilaments marked by arrowheads *2* and *3* bears a double-headed globule near its center (asterisk *3*). Finally, in the far right side of this field, a globular mass, ~15 nm in diameter, sits on crossed spectrin filaments (asterisk *4*). This could be two ankyrins on a band 3 oligomer linking two spectrin tetramers, which run between four different actin protofilaments. Thus, ankyrin/band 3 complexes may not only couple spectrin to the bilayer (4, 5, 10, 17) but may also join spectrin tetramers to one another near their centers. Bivalent ankyrin/band 3 complexes may thus provide a second spectrin linkage system complementary to that of actin/band 4.1. Of course, positive identification of each protein in these complexes is needed and is being studied.

The spectrin/actin binding ratio provides a check on the validity of our interpretation of the images we obtained of the intact skeleton. Estimates in the literature suggest that there is one spectrin dimer for every 1.0–2.5 actin monomers in the ghost (15, 31, 38, 43). These figures correspond to the joining of ~5–12 spectrin ends to each 33 nm, 12-subunit actin protofilament. Figs. 3, *c–e*, 4, and 6 suggest that five is a lower limit and perhaps eight is an upper limit for this binding ratio. The agreement between the biochemical and microscopic analysis is satisfying.

The skeleton of the human red cell membrane is so dense a structure that its native molecular organization has yet to be analyzed directly by electron microscopy. We have therefore explored ways to increase the visibility of the elements in the intact skeleton and the connections among them while preserving their essential organization. The experimental variable most useful to us in this regard has been the manipulation of ionic strength.

Concluding Comments

High ionic strength buffers strip skeletons of their accessory proteins. What remains are their basic or essential components (i.e., those without which the integrity of the skeleton would be lost): spectrin, actin, and band 4.1 (37). The stripped skeleton has been a valuable starting point for visualizing the organization of the intact network (see Fig. 2 and reference 39). However, significant structural alterations may attend its preparation. In particular, skeletons became highly condensed when exposed to the molar salt solutions required to strip them of accessory proteins. Their re-expansion required prolonged dialysis against very dilute buffers. As discussed above, actin monomers may migrate in this destabilizing environment, extending some filaments at the expense of others. Furthermore, the removal of accessory proteins, bands 2.1 and 3 as well as actin-binding proteins such as tropomyosin (16) and band 4.9 (41), risks altering ultrastructure significantly.

Low ionic strength, alkaline buffers have two kinds of effects on the molecular organization of the skeleton: reversible expansion and irreversible breakdown. The former is manifested by the swelling of skeletons at low ionic strength (19, 23). This dilation is requisite to our ultrastructural analysis. The irreversible effects of low ionic strength on the skeleton involve the progressive dissociation of its constituent proteins, particularly at 37°C. As spectrin tetramers dissociate to dimers (25, 34, 50) and actin protofilaments depolymerize to monomers (22, 31), the skeleton as a whole is reduced to fragments (2, 23, 39) and ultimately to its protein subunits. While we have previously exploited controlled fragmentation to increase the visibility of the components of the skeleton (39), we now seek the benefits of reversible expansion without the loss of native organization brought about by protein dissociation.

The micrographs in Fig. 3 encourage the hypothesis that

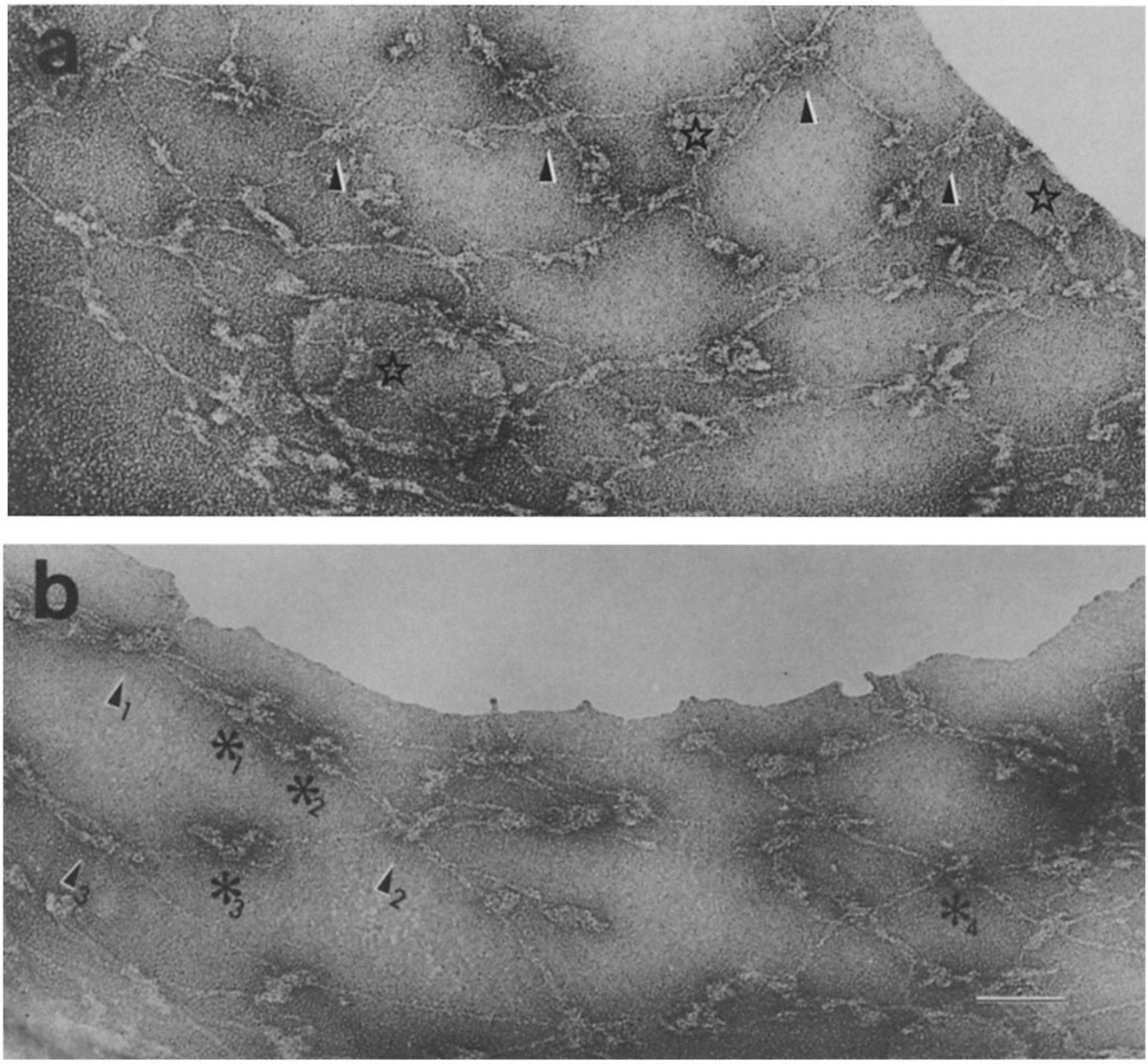

Figure 6. The unstripped red cell skeleton: expansion by washing with water on a fenestrated film. A carbon film identical to that shown in Fig. 3, *c–e* was perfused for 15 s with a stream of distilled water at room temperature before staining with uranyl acetate. The stars indicate liquid plaques, the arrowheads indicate actin protofilaments, and the asterisks indicate four globular complexes on spectrin filaments. Bar, 50 nm.

spectrin may not be in an elongated form in the native skeleton but condensed, presumably through weak intramolecular and/or intermolecular interactions which are reversed by electrostatic repulsion at low ionic strength. The fact that the skeleton can be expanded to an area a few times greater than that of the membrane itself (see above and reference 23) also suggests that spectrin is not fully extended in situ. Furthermore, it can readily be calculated that the average distance between uniformly distributed actin protofilaments on the membrane is about one-third the length of the fully extended spectrin tetramer. Since we have observed no tendency for spectrin filaments to cross or extend beyond the most proximal actins, their form in situ is likely to be condensed and/or convoluted.

The condensed structures in Fig. 3 open in a characteristic fashion: thick amorphous conglomerates give way to thin, linear segments which are recognizable as spectrin. Progressive expansion seems to reflect an increase in both the length of the linear segments and their frequency. While the structure of the conglomerates is unknown, it seems that they are not simply precipitates caused by the negative stain or other manipulations, since the images vary systematically with the conditions of preparation. Furthermore, the long incubation time required to turn conglomerates into filaments suggests that they are stable structures. The idea of reversible cohesion among flexible elements in the skeleton is also supported by studies on the thermoelasticity of the intact red cell membrane (51).

While the spectrin filaments in our micrographs vary both in length and in width, the negative staining technique does

not permit us to determine whether these parameters are inversely related and reflect the unfolding process. Even in the most highly expanded skeletons (eg., Figs. 2 and 6), spectrin filaments, while highly elongated, rarely approach 200 nm in length. This bespeaks a propensity for spectrin to condense by intramolecular self-association, a potential that could be strongly realized in vivo. Skeletons released into isotonic saline assume a surface area smaller than the parent membrane (9, 19, 23), suggesting that the network is held open in situ through association with multiple anchor proteins in the bilayer.

The predominant skeleton-building form of spectrin in vivo appears to be an $(\alpha\beta)_2$ tetramer of molecular weight $\sim 10^6$ (21, 40). Since spectrin is both highly acidic and flexible, its Stokes radius varies inversely and reversibly with ionic strength (32, 44). These features allow the shape of the purified tetramer to range widely, from a moderately asymmetrical compact form (20) to an expanded and more symmetrical flexible coil of Stokes radius ~20 nm (33, 44) to a flexible thin filament that can be drawn out to 194 nm in length (40). These excursions in folding may reflect segmental rearrangements within the molecule rather than denaturation (32, 33). Specifically, it has been proposed that spectrin polypeptides are folded into multiple stable domains, each ~12,000 in molecular weight, joined by short disordered regions (42). The electrostatic expansion of the skeleton may involve the separation of these hinged domains from a compact, associated state assumed in the conglomerates.

We are reluctant to interpret the molecular organization and dynamics of the intact skeleton in terms of what is known at present about isolated spectrin. Spectrin is universally solubilized in very dilute, alkaline buffers. We do not know whether its native folding pattern is preserved under those conditions or can be recovered upon return to physiological media. There is evidence, for example, that warming tetrameric spectrins in 5 mM NaP_i at pH 7.5 leads to irreversible changes in their conformation (Fig. 5 in reference 35). Furthermore, the fact that solubilized spectrin aggregates laterally into fibrous bundles when incubated in millimolar dilvalent cation solutions (36, 47) suggests that the isolated spectrin may have undergone irreversible unfolding in vitro. Therefore, a consensus on the behavior of spectrin isolated in low ionic strength solutions may not immediately guide us to its structure in vivo.

It has recently been argued from hydrodynamic studies on isolated spectrin that the skeleton may behave as a gel of randomly coiled ionic elastomers with little or no stable structure within or among the chains (45). Can this hypothesis be reconciled with the kinetic stability (i.e., slow expansion) of the condensed skeleton and the compact structures seen in Fig. 3? Gels composed of charged polymers are known to undergo sharp phase transitions between condensed and expanded states as a function of ambient conditions such as ionic strength (46). The expansion of the skeleton observed in Fig. 3 could represent such a change in state. It will be important to establish whether the elasticity of the skeleton in vivo results from specific folding (51) or nonspecific condensation (45) of the elongated spectrin molecules.

In conclusion, we have yet to visualize the native skeleton in the erythrocyte, but we have been able to reduce the perturbations required to gather useful information about it. An immediate challenge is to prepare spectrin and other fractions of the skeleton in a form that is both more native and more visible than heretofore.

After the submission of our manuscript, Byers and Branton (8) published an elegant ultrastructural study on the association of proteins in the erythrocyte membrane skeleton. Their major findings agree with our own.

The authors wish to thank Mr. Sang Jen Suh and Mr. Gerald Groffman for their excellent technical assistance.

This work was supported by American Heart Association Grant 81-664 (to B. W. Shen), American Cancer Society Grant BC-95 (to T. L. Steck), and National Institutes of Health Grants HL 33254 (to B. W. Shen), HL 22654 (to R. Josephs), and HL 30121.

Received for publication 12 September 1985, and in revised form 7 November 1985.

References

1. Anderson, R. A., and R. E. Lovrien. 1984. Glycophorin is linked by band 4.1 protein to the human erythrocyte membrane skeleton. *Nature (Lond.)*. 307:655–658.

2. Beaven, G. H., L. Jean-Baptiste, E. Ungewickell, A. J. Baines, F. Shahbakhti, J. C. Pinder, S. E. Lux, and W. B. Gratzer. 1985. An examination of the soluble oligomeric complexes extracted from the red cell membrane and their relation to the membrane skeleton. *Eur. J. Cell Biol.* 30:299–306.

3. Beaven, G. H., and W. B. Gratzer. 1980. Interaction of divalent cations with human red cell cytoskeletons. *Biochem. Biophys. Acta.* 660:140–149.

4. Bennett, V. 1982. The molecular basis for membrane-cytoskeleton association in human erythrocyte. *J. Cell. Biochem.* 18:49–65.

5. Bennett, V. 1985. The membrane skeleton of human erythrocytes and its implications for more complex cells. *Annu. Rev. Biochem.* 54:273–304.

6. Branton, D., C. M. Cohen, and J. Tyler. 1981. Interaction of cytoskeletal proteins on the human erythrocyte membrane. *Cell.* 24:24–32.

7. Brenner, S. L., and E. D. Korn. 1980. Spectrin-actin complex isolated from sheep erythrocytes accelerates actin polymerization by simple nucleation: evidence for oligomeric actin in the erythrocyte cytoskeleton. *J. Biol. Chem.* 255:1670–1676.

8. Byers, T. J., and D. Branton. 1985. Visualization of the protein associations in the erythrocyte membrane skeleton. *Proc. Natl. Acad. Sci. USA.* 82:6153–6157.

9. Canham, P. B. 1970. The minimum energy of bending as a possible explanation of the biconcave shape of the human red blood cell. *J. Theor. Biol.* 26:61–81.

10. Cohen, C. 1983. The molecular organization of the red cell membrane skeleton. *Semin. Hematol.* 20:141–158.

11. Cohen, C. M., J. M. Tyler, and D. Branton. 1980. Spectrin-actin associations studied by electron microscopy of shadowed preparations. *Cell.* 21:875–883.

12. Cohen, C. M., and R. C. Langley, Jr. 1984. Functional characterization of human erythrocyte spectrin a and b chains: association with actin and erythrocyte protein 4.1. *Biochemistry.* 23:4488–4495.

13. Côté, G. P. 1983. Structural and functional properties of the non-muscle tropomyosins. *Mol. Cell. Biochem.* 57:127–146.

14. Egelman, E. H., N. Francis, and D. D. DeRosier. 1982. F-actin is a helix with a random variable twist. *Nature (Lond.)*. 298:131–135.

15. Fairbanks, G., T. L. Steck, and D. F. H. Wallach. 1971. Electrophoretic analysis of the major polypeptides of the human erythrocyte membrane. *Biochemistry.* 10:2606–2617.

16. Fowler, V. M., and V. B. Bennett. 1984. Erythrocyte membrane tropomyosin. Purification and properties. *J. Cell Biol.* 259:5978–5988.

17. Goodman, S. R., and K. Shiffer. 1983. The spectrin membrane skeleton of normal and abnormal human erythrocytes: a review. *Am. J. Physiol.* 244:C121–C141.

18. Hainfeld, J., and T. L. Steck. 1977. The sub-membrane reticulum of the human erythrocyte: a scanning electron microscopic study. *J. Supramol. Struct.* 6:301–317.

19. Johnson, R. M., G. Taylor, and D. B. Meyer. 1980. Shape and volume changes in erythrocyte ghosts and spectrin-actin networks. *J. Cell Biol.* 86:371–376.

20. Kam, Z., R. Josephs, H. Eisenberg, and W. B. Gratzer. 1977. Structural study of spectrin from human erythrocyte membranes. *Biochemistry.* 16:5568–5572.

21. Knowles, W., S. L. Marchesi, and V. T. Marchesi. 1983. Spectrin: structure, function, and abnormalities. *Semin. Hematol.* 20:159–174.

22. Korn, E. D. 1982. Actin polymerization and its regulation by proteins from non-muscle cells. *Physiol. Rev.* 62:672–737.

23. Lange, Y., R. A. Hadesman, and T. L. Steck. 1982. Role of the reticulum in the stability and shape of the isolated human erythrocyte membrane. *J. Cell*

Biol. 92:714–721.

24. Lin, D. C., and S. Lin. 1978. High affinity binding of [^{3}H]-dihydrocytochalasin B to peripheral membrane proteins related to the control of cell shape in the human red cell. *J. Biol. Chem.* 253:1415–1419.

25. Liu, S. C., and J. Palek. 1980. Spectrin tetramer-dimer equilibrium and the stability of erythrocyte membrane skeletons. *Nature (Lond.).* 285:586–588.

26. Liu, S. C., P. Windisch, S. Kim, and J. Palek. 1984. Oligomeric states of spectrin in normal erythrocyte membranes: biochemical and electron microscopic studies. *Cell.* 37:587–594.

27. Matsumura, F., S. Yamashiro-Matsumura, and J. Jung-Ching Lin. 1983. Isolation and characterization of tropomyosin-containing microfilaments from cultured cells. *J. Biol. Chem.* 258:6636–6644.

28. Mueller, T. J., and M. Morrison. 1981. Glycoconnectin (PAS-2), a membrane attachment site for the human erythrocyte cytoskeleton. *In* Erythrocyte Membranes 2: Recent Clinical and Experimental Advances. W. Kruchberg, J. Eaton, and G. Brewer, editors. Alan R. Liss, New York. 95–112.

29. Nermut, M. V. 1981. Visualization of the "membrane skeleton" in human erythrocytes by freeze-etching. *Eur. J. Cell Biol.* 25:265–271.

30. Ohanian, V., L. C. Wolfe, K. M. John, J. C. Pinder, S. E. Lux, and W. B. Gratzer. 1984. Analysis of the ternary interaction of the red cell membrane skeletal proteins: spectrin, actin, and band 4.1. *Biochemistry.* 23:4416–4420.

31. Pinder, J. C., and W. B. Gratzer. 1983. Structure and dynamic states of actin in the erythrocyte. *J. Cell. Biol.* 96:768–775.

32. Ralston, G. B. 1976. The influence of salt on the aggregation state of spectrin from bovine erythrocyte membranes. *Biochim. Biophys. Acta.* 443:387–393.

33. Ralston, G. B. 1976. Physico-chemical characterization of the spectrin tetramer from bovine erythrocyte membranes. *Biochim. Biophys. Acta.* 455:163–172.

34. Ralston, G. B., J. Dunbar, and M. White. 1977. The temperature-dependent dissociation of spectrin. *Biochim. Biophys. Acta.* 491:345–348.

35. Ralston. G. B. 1978. Physical-chemical studies of spectrin. *J. Supramol. Struct.* 8:361–373.

36. Rosenthal, A. S., F. M. Kregenow, and H. L. Moses. 1970. *Biochim. Biophys. Acta.* 196:254–262.

37. Sheetz, M. P. 1979. Integral membrane protein interaction with triton cytoskeletons of erythrocytes. *Biochim. Biophys. Acta.* 557:122–134.

38. Shelton, R. L., Jr., and R. G. Langdon. 1984. Quantitation of the major proteins of the human erythrocyte membrane by amino acid analysis. *Anal. Biochem.* 140:366–371.

39. Shen, B. W., R. Josephs, and T. L. Steck. 1984. Ultrastructure of unit fragments of the skeleton of the human erythrocyte membrane. *J. Cell Biol.* 99:810–821.

40. Shotton, M. D., B. E. Burke, and D. Branton. 1979. The molecular structure of human erythrocyte spectrin. Biophysical and electron microscopic studies. *J. Mol. Biol.* 131:303–329.

41. Siegel, D. L., and D. Branton. 1985. Partial purification and characterization of an actin-bundling protein, band 4.9, from human erythrocytes. *J. Cell Biol.* 100:775–785.

42. Speicher, D. W., and V. T. Marchesi. 1984. Erythrocyte spectrin is comprised of many homologous triple helical segments. *Nature (Lond.).* 311:177–180.

43. Steck, T. L. 1974. The organization of proteins in the human red blood cell membrane. *J. Cell Biol.* 62:1–19.

44. Stokke, B. T., and A. Elgsaeter. 1981. Human spectrin. 6. A viscometric study. *Biochim. Biophys. Acta.* 640:640–645.

45. Stokke, B. T., A. Mikkelsen, and A. Elgsaeter. 1985. Human erythrocyte spectrin dimer intrinsic viscosity: temperature dependence and implications for the molecular basis of the erythrocyte membrane free energy. *Biochim. Biophys. Acta.* 816:102–110.

46. Tanaka, T. 1981. Gels. *Sci. Am.* 244:124–138.

47. Tilney, L. G., and P. Detmers. 1975. Actin in erythrocyte ghosts and its association with spectrin. Evidence for a nonfilamentous form of these molecules in situ. *J. Cell Biol.* 66:508–520.

48. Timme, A. H. 1981. The ultrastructure of the erythrocyte cytoskeleton at neutral and reduced pH. *J. Ultrastruct. Res.* 77:199–209.

49. Tsukita, S., S. Tsukita, and H. Ishikawa. 1980. Cytoskeleton network underlying the human erythrocyte membrane. Thin section electron microscopy. *J. Cell Biol.* 85:567–576.

50. Ungewickell, E., and W. Gratzer. 1978. Self-association of human spectrin: a thermodynamic and kinetic study. *Eur. J. Biochem.* 88:379–385.

51. Waugh, R., and E. Evans. 1979. Thermoelasticity of red blood cell membranes. *Biophys. J.* 26:115–132.

52. Yu, J., D. A. Fischman, and T. L. Steck. 1973. Selective solubilization of proteins and phospholipids from red blood cell membranes by nonionic detergent. *J. Supramol. Struct.* 1:233–248.

53. Yu, J., and T. L. Steck. 1975. Associations of band 3, the predominant polypeptide of the human erythrocyte membrane. *J. Biol. Chem.* 250:9176–9184.